Journal of Materials Chemistry B

Accepted Manuscript

ROYAL SOCIETY OF CHEMISTRY

www.rsc.org/materialsB

RSCPublishing

ARTICLE

Solid Supported Lipid Bilayers from Artificial and Natural Lipid Mixtures – Long-term Stable, Homogeneous and Reproducible

I. Möller[a], Stefan Seeger[b,*]

Cite this: DOI: 10.1039/x0xx00000x

Received ooth January 2012,
Accepted ooth January 2012

DOI: 10.1039/x0xx00000x

www.rsc.org/

Supported lipid bilayers (SLBs) are increasingly accepted as experimental models to study the behaviour of membrane active proteins like α-Synuclein, as they can easily be investigated by surface sensitive analytical methods. In this study we show the assembly and long-term stability of SLBs on glass substrates by vesicle deposition from various lipid mixtures. For the investigation of the SLBs we use Supercritical Angle Fluorescence Microscopy and Spectroscopy. We concentrate on the important factors for reproducible bilayer assembly like the purification of the substrate and the handling of the lipid vesicle suspension. By using a new combined steady-state/flow approach we were able to create homogeneous SLBs with a long-term stability over seven days, which to our knowledge have not been reported in literature so far, including SLBs containing up to 70 % negatively charged lipids, SLBs from artificial lipid mixtures containing cholesterol as well as SLBs from natural lipid extracts.

1. Introduction

Artificial lipid bilayers in any form are important systems to mimic cell membranes and are extensively used in research to investigate processes at the level of the membrane without interference of the cell body. By using simplified lipid systems specific problems can be addressed and resolved more clearly. Artificial lipid bilayers are used to study membrane proteins like gramicidin D[1] or the interaction of membrane active proteins like α-Synuclein[2–5] with certain lipids inside the bilayer and are important for the development of new biosensors.[6] Many applications demand for a differentiation between events in the solution and events on the lipid bilayer. Apart from that, especially in assays with amyloidogenic proteins, the curvature of the lipid bilayer has to be homogeneous.[7] In these cases liposomes, which are often used due to the simplicity of their production,[8] e.g. in Tryptophan fluorescence assays,[9] are unsuitable. The widely applied lipid film hydration method for these liposomes produces vesicles of different sizes: While the big vesicles are standardized to a certain size by extrusion, smaller vesicles stay unaffected.[10] Also the localization of events happening is not possible.

By using solid supported lipid bilayers (SLBs) both effects are ruled out. A SLB provides a flat bilayer, which can be easily addressed by surface sensitive methods like surface plasmon resonance,[11] quartz crystal microbalance,[12] atomic force microscopy[13] or supercritical angle fluorescence (SAF) microscopy.[4] Several protocols for the formation of SLBs exist. The first one is based on the Langmuir-Blodgett technique, where the SLB is established by dipping the substrate into a Langmuir trough.[14] The drawback of this approach is that the SLB cannot be built up in a closed measuring cell. The transfer though of the pre-assembled bilayer on a substrate into a closed measuring cell that allows the complete exchange of buffers and the application of a protein solution with a defined concentration is demanding. Another way to build up a SLB is the vesicle fusion method.[15] Preformed vesicles are adsorbed on a solid support and subsequently ruptured by treatment with fusogenic agents to form the SLB. This method can be applied to hydrophilic and hydrophobic surfaces by help of an amphiphilic α-helical fusion peptide.[16 18] While this method has the advantage to be suitable to a broad range of substrates, its drawbacks are the high cost and difficult handling of the fusogenic agent compared to e.g. earth alkaline salts like $CaCl_2$. These can be used for bilayer assembly on hydrophilic surfaces and are there preferred due to their operation simplicity. The preferred support materials are glass[17] and other SiO_2-based materials like mica.[19] Uncharged SLBs made of PC are easily formed and are widely used in the literature.[17 20 21] The formation of negatively charged PS containing SLBs though is more demanding. The adsorption and rupture of the vesicles in this case has to be triggered with divalent cations like Ca^{2+}. Procedures for the assembly of SLBs with a PS content of up to 20 %[22 23] have been described. Protocols using a higher PS content are only known for mica substrates.[24] Besides the problem, that with high PS content the vesicles do not always

rupture and the SLB is susceptible for defects, also long-time instability caused by a destabilization of the SLB by Ca^{2+} is an issue.[25] As natural membranes contain around 37 % of charged phospholipids,[26] incorporating a higher PS content is important. Richter et al. solved this problem for mica substrates by the removal of Ca^{2+} with EDTA. This leads not only to enhanced stability of the SLB, but also to a restructuration and homogenisation of the SLB.[25]

As assays based on SLBs are more and more common, herein we show the assembly of stable SLBs from a large variety of lipid mixtures providing long-term stability that has not been yet reported. We use supercritical angle fluorescence microscopy and spectroscopy to investigate the structure and the dynamics of the SLB.[27] [28] Furthermore, we address obstacles which can occur during SLB formation. The development of a defined flow/steady state sequence in combination with careful pre-treatment of the glass substrate, enabled us to build up long-time stable, defect-free SLBs even with a PS content up to 70 %. Additionally, we were able to create SLBs from natural lipid extracts. All SLBs reported here showed a long-time stability of more than seven days. In summary we cannot only mimic membranes, but we are now also able to rebuild natural membranes, which can be studied with high reproducibility without interference of intracellular processes over prolonged time spans.

2. Experimental

2.1 Materials

1,2-Dioleoyl-sn-glycero-3-phospho-L-serine sodium salt (DOPS), 1,2-dioleoyl-sn-glycero-3-phosphocholine (DOPC) and lipid extracts as solutions in chloroform were purchased from Avanti® Polar Lipids, Inc. (Alabaster, USA) and used as received. Atto647-labeled and Atto647N-labeled 1,2-dioleoyl-sn-glycero-3-phosphoethanolamine (Atto647-DOPE and Atto647N-DOPE, head group labeled) was purchased from Atto-Tec GmbH (Germany) and dissolved in chloroform to a concentration of 0.8 µg/mL before use. CellMask™ Deep Red Plasma membrane Stain (CellMask) was purchased from Thermo Fisher Scientific Inc (USA). Phosphate buffered saline (PBS) buffer was purchased from Sigma-Aldrich® (Switzerland), adjusted to pH 7.4 and treated with NaN_3 (5 % w/w in water) to a final azide concentration of 0.05 % w/w. Glass slides were purchased as coverslips from Menzel-Gläser, Gerhard Menzel GmbH (Germany). Plastik 70 was purchased from Kontaktchemie, CRC Industries GmbH (Germany). The glue Loctite 3311 was purchased from Henkel (Germany).

2.2 Measurement setup.

The SLB was formed out of vesicles under combined flow/steady-state conditions in a closed measuring cell, consisting of a glass slide, which was glued on a measuring cell with in- and outlet for the flow.

2.3 Preparation of artificial lipid vesicles

DOPC, DOPS and cholesterol in chloroform were mixed in a glass test tube at the desired mass ratio to a final lipid amount of 0.5 mg. Headgroup labelled Atto647-DOPE or Atto647N-DOPE in chloroform was added at a mass ratio of 1:62 500. The chloroform was evaporated in a nitrogen stream and remaining chloroform and traces of water were removed in the lyophilizer overnight. The dried lipids were dissolved in tris(hydroxymethyl)aminomethane (Tris) buffer with Ca^{2+} (10 mM Tris, 5 mM $CaCl_2$, 149 mM NaCl, 0.05 % NaN_3, pH 7.4, 1.0 mL), vortexed and extruded 29 times through a polycarbonate membrane (0.1 µm pore size). The final lipid suspension was diluted with Tris buffer with Ca^{2+} to a concentration of 0.1 mg/mL and used immediately.

2.4 Preparation of lipid vesicles from natural tissue lipid extracts

The natural lipid extract (0.5 mg) in chloroform was mixed with Atto647-DOPE in chloroform at a mass ratio of 1:62 500. The chloroform was evaporated in a nitrogen stream and remaining chloroform and traces of water were removed in the lyophilizer overnight. The dried lipids were dissolved in water to give a final concentration of 1 mg/mL by heating them to 65 °C for 30 min, vortexed and extruded 29 times through a polycarbonate membrane (0.1 µm pore size). During extrusion the temperature of the lipid solution was kept above the phase transition temperature. The final lipid suspension was diluted with Tris buffer with Ca^{2+} to a concentration of 0.1 mg/mL and used immediately.

2.5 Preparation of the glass slide and the measuring cell

Glass slides were cleaned by ultrasonification in ethanol for 15 min and stored under ethanol until usage. Directly before usage the slides were treated with oxygen plasma to ensure cleanliness and an improved hydrophilicity. The measuring cell was cleaned with Deconex Cip7, ethanol and water for 15 min by ultrasonification each. The measuring cell was coated with Plastik 70 and let dry for 50 min, to ensure a scratch free, clean and reproducible surface on a large variety of materials.

After the preparation of the measuring cell and the glass slide, they were glued together with Loctite 3311 and filled immediately with Tris buffer with Ca^{2+}.

2.6 Preparation of SLBs

For the SLB preparation a protocol based on Richter's work on mica surfaces was used.[25] First, the lipid suspension was applied with a flow of 0.250 mL/min over 10 min before stopping the flow for a certain time *t* (dependent on the lipid mixture, see 3.1, 3.3-3.4) to allow vesicle deposition. The established SLB was rinsed with Tris buffer with Ca^{2+} for 15 min and subsequently with Tris buffer with EDTA (10 mM Tris, 5 mM EDTA, 133 mM NaCl, 0.05 % NaN_3, pH 7.4) for 16 min. After washing, the buffer was changed to PBS buffer for the rest of the measurement.

2.7 SAF microscopy and fluorescence correlation spectroscopy (FCS)

Images of the labelled SLBs were taken by scanning an area of 37.5 µm x 37.5 µm (slow scanning direction in y-direction with a total scan time of 6 min) using the SAF setup described by Ruckstuhl et al.[29 30] The obtained images were processed with Matlab (Mathworks®, USA). FCS measurements of the labelled lipids in the SLB were also conducted with the SAF setup.[29] The obtained curves were fitted with a two-dimensional model[27](D_1 fit):

$$G(\tau) = G_0 * \frac{1}{1 + 4\,{}^{D}\!/_{\omega_0^2} * \tau}$$

Eq. 1

with G_0 being the y-intercept of the FCS-curve, inversely proportional to the number of fluorescent molecules, ω_0 being the $1/e^2$ radius of the detection volume and D the diffusion coefficient of the labeled lipids inside the SLB.

In some cases, this model was expanded with a second diffusion coefficient (D_2 fit), resulting in the formula:

$$G(\tau) = a * G_0 * \frac{1}{1 + 4\,{}^{D_a}\!/_{\omega_0^2} * \tau} + b * G_0 * \frac{1}{1 + 4\,{}^{D_b}\!/_{\omega_0^2} * \tau}$$

Eq. 2

with

$$D = a * D_a + b * D_b \quad and \quad a + b = 1.$$

Eq. 3

3. Results and discussion

3.1 SLBs from artificial lipid mixtures

We report the assembly of SLBs from artificial lipid mixtures containing DOPC and DOPS in various ratios. With the procedure described above, mole fractions of DOPS x_{DOPS} of up to 0.7 can be achieved. To the best of our knowledge, this is the first report of flow-stable SLB systems that contain this level of net charged lipids.

Typically, SLB formation starts with vesicle deposition on the solid support. After a sufficient vesicles coverage, the vesicles rupture and fuse to a SLB. The steady state time t, until the SLB is completely formed, is dependent on the content of DOPS x_{DOPS} in the lipid mixture and can be described by an exponential increase (Fig. 1) (As a rule of thumb t=15 min is enough for lipid compositions of up to x = 0.4). For the systems investigated in this work, the number of vesicles adsorbed in time, visible as bright red-yellow spots in the SAF scan, is independent from the lipid ratio (Fig.2a und b). Once a critical coverage is reached, vesicle rupture starts to form the SLB. Our flow/steady state sequence in combination with the SAF technique enables us to carefully monitor vesicle deposition and to ensure sufficient surface coverage. Hence, eventually occurring incomplete vesicle deposition in mixtures containing high levels of DOPS which leads to defects in the SLB and lipid aggregates can easily be identified and avoided.

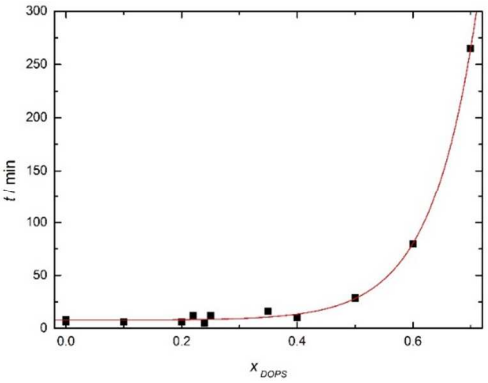

Figure 1. Time of vesicle disruption as function of the concentration of DOPS x_{DOPS} in the lipid vesicles.

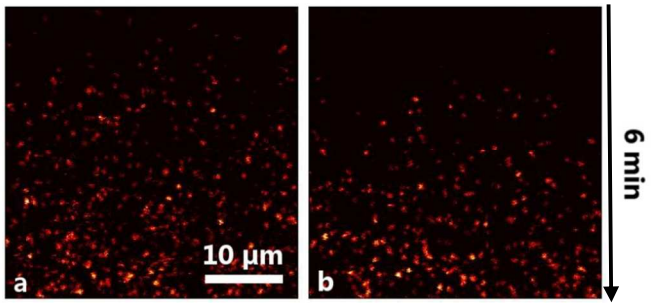

Figure 2. Images of the vesicle deposition 2 min before until 4 min after start of incubation from a vesicle suspension with 100 % DOPC **(a)** and DOPC/DOPS 50:50 **(b)**. The images are obtained by scanning (slow scanning direction in y-direction) with a total scan time of 6 min.

DOPC SLBs can easily be assembled already at low surface coverage, while the coverage has to be much higher for SLBs consisting of DOPC and DOPS (*e.g.* 50:50, Fig. 3a and b) resulting in a higher lipid density in the SLB. This is in line with the proposed model of Richter et al., where the disruption process can follow two pathways depending on vesicle charge implying that highly charged vesicles need full surface coverage to trigger the rupture process.[25]

With a too short steady state incubation time this full surface coverage cannot be achieved. This can lead to defects and lipid aggregates on highly negatively charged SLBs. The SLB formation with a DOPS content up to $x = 40$ % is very robust though (deviation of 20 % on the perfect time point does not disturb SLB formation, stability or homogeneity), as a full vesicle coverage is not needed.

The formation of the bilayer does not occur via bilayer patches, but by a sudden rupture (Fig. 3a and b). The change of a vesicle layer to a SLB can be detected by an enhanced homogenisation, as well as a loss of visible structures (lipid vesicles). As the lipids now freely diffuse, they can be resolved in the fast scanning direction, but not in the slow scanning direction anymore, resulting in parallel linear structures in the SAF scans. The change from vesicle layer to SLB can also be shown by the reduction of the Pearson correlation coefficient (PCC) between all consecutive scanned lines [31] (Fig. 3c and d). As the vesicles cover several lines, a strong correlation between the lines can be observed. For the SLB no or only little correlation can be detected due to the missing resolution in the slow scanning direction.

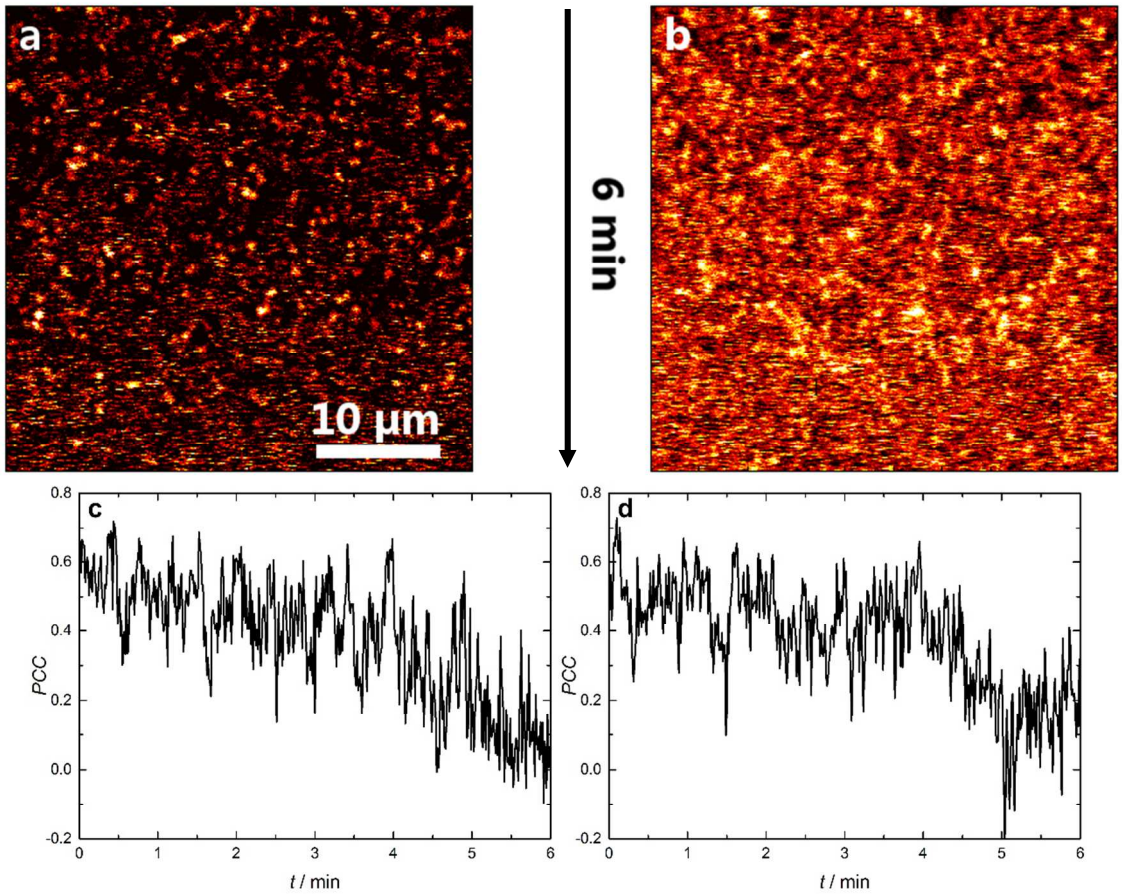

Figure 3. SAF scans of the rupture of the vesicles into a SLB for DOPC 100 % **(a)** and DOPC/DOPS 50:50 **(b)** with lipid vesicle layer (upper part) and emerging SLB (lower part). To show the difference between vesicle layer and bilayer, the PCC of consecutive scanned lines was plotted against the scanning time for 100 % DOPC **(c)** and DOPC/DOPS 50:50 **(d)**.

After the steady state incubation and the complete formation of the SLB, unruptured vesicles and small defects are visible (Fig. 4, blue box) and the SLB is still unstable. To get a fully homogenous and long-term stable SLB, several rinsing steps are necessary. After removing undisrupted lipid vesicles with Tris buffer with Ca^{2+}, the SLB is rinsed with Ca^{2+} complexing EDTA containing Tris buffer. Ca^{2+} is destabilizing lipid vesicles and SLBs by intercalating between lipid headgroups and therefore triggers the lipid vesicle disrupture.[32] So while it is indispensable for SLB formation, for SLB stability it is counterproductive.

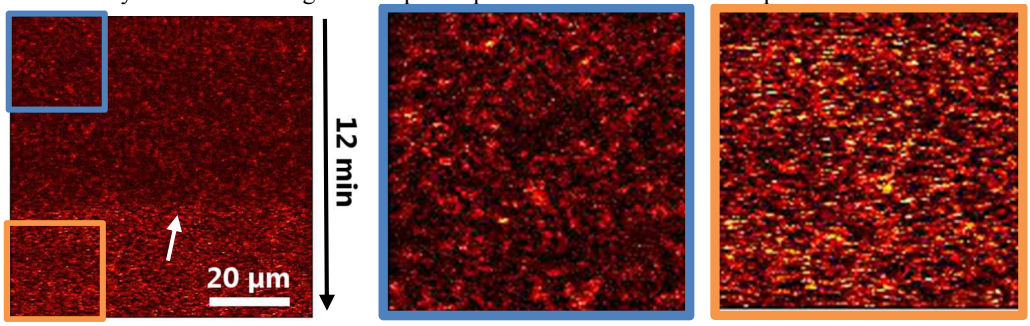

Figure 4. SAF image of a DOPC/DOPS 65:35 SLB with an enlarged detail of the SLB before (blue box) and after (orange box) washing with EDTA. The effect is visible directly after the first contact of the SLB with the EDTA containing buffer. The arrow shows the beginning of the restructuration.

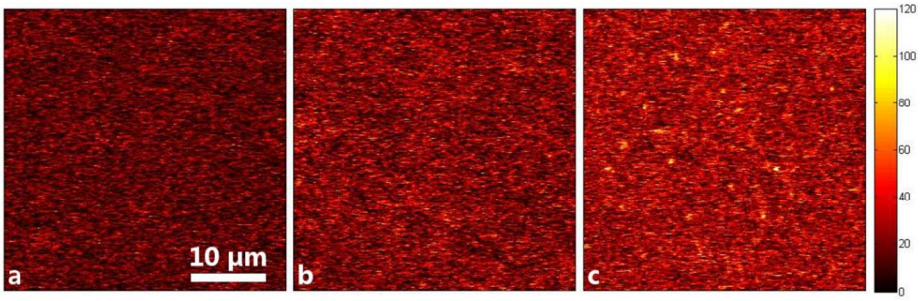

Figure 5. SLBs after 30 min after washing with EDTA with **(a)** 100 % DOPC, **(b)** DOPC/DOPS 65:35 and **(c)** DOPC/DOPS 40:60. By washing with EDTA a disruption of remaining vesicles as well as a fast restructuration and healing of small defects is observed leading to high SLB homogeneity and stability (Fig. 4, orange box). A clear change in morphology is visible in the SAF scan(see arrow, Fig. 4).Therefore we conclude that EDTA binds Ca2+ leading to a release of Ca2+ ions intercalated between the headgroups of the lipids. This bilayer restructuration is also described by Richter et al.[25] Homogenous SLBs with different contents of DOPS up to 70 % have been obtained by EDTA treatment, SAF scans of exemplary SLBs are shown in Fig. 5.

3.2 Factors for successful SLB assembly

The formation, homogeneity and the stability of the SLB are dependent on various factors like lipid composition, properties of the glass slide, buffers etc. In this section, we present investigations of the most important factors for successful SLB assembly.

3.2.1 Purification of the glass surface Prior to SLB formation, the solid support, here the glass slide, has to be cleaned carefully. In most protocols published so far, detergents like Hellmanex,[20] SDS,[25] or Piranha[33] are used. However, the use of these detergents leads to a change in the ζ-potential of the glass surface.[34] Even after rinsing the slides with water afterwards, the surface properties could not be prepared in a reproducible manner (Fig. 6).

To show the influence of different cleaning procedures on the properties of the glass surface and the emerging bilayer, SLBs with DOPC 100 % and the negatively charged Atto647N-DOPE were built up on differently cleaned glass slides.

As cleaning agents of choice highly acidic Piranha (P) and Deconex 11, a highly basic detergent, were used. For Deconex 11 additionally the rinsing procedure with water after the detergent treatment was varied: 15 min in ultrasonic bath (Dec_u), rinsing with water (~15 mL, Dec_n) or short dipping in water (Dec_s). The obtained SLBs were analysed with SAF-FCS (Fig. 6a and b). From this analysis information about the SLB density as well as the diffusion inside the SLB are gained. Evaluation of G_0, which is inversely proportional to the number of fluorescent molecules and hence an indirect measure of the lipid density in the SLB, shows that the SLBs P, Dec_u, and Dec_n show a comparable high lipid density. Only the SLB Dec_s has a lower lipid density, which can be explained by a contamination of the surface with the detergent due to insufficient rinsing.

All FCS curves were fitted with the D_1 and D_2 fit. For SLBs P and Dec_u it is obvious from the graph, that the D_1 fit does not match the measured data (Fig. 6c). The resulting diffusion coefficients are depicted in Table 1.

All models were tested with a F-test.[34,35] This test compares the fits with two nested models, i.e. one model being a simplified version of the other one. It determines, if the loss of degrees of freedom (due to more parameters) is compensated by an improved quality of the fit. Only for Dec_n the better model, according to the F-test, is the D_1 model. This fits with the observation that no meaningful result is obtained from the D_2 fit in this case. Although the F-test determines D_2 to fit best the remaining datasets, the result for Dec_s with the D_2 fit is questionable. In this case, the errors for D_b, as well as for the coefficient a are extremely high. Hence, $a = 100$ % lies within the error range. In this case, b would be 0 and the D_2 model would converge with the D_1 model. Therefore the D_1 model cannot be excluded with the F-test and a clear decision for one model cannot be drawn.

The second diffusion coefficient reflects a difference between the two layers of the SLB. While the lipid molecules in the upper layer can move freely in the layer, the bottom layer interacts with the glass surface and therefore the diffusion is most likely hindered. This is also supported by the fact, that the weighted average of the diffusion coefficient is lower in these cases. However, Przybylo et al. discovered, that this interaction with the substrate is weaker than the interaction between the layers resulting in an equal lipid diffusion in both leaflets.[36] For their studies though they used mica substrates. There are also studies on silica beads, which observe the same effect as we do.[37] Therefore we conclude, that this effect is also strongly dependent on the type of the substrate.

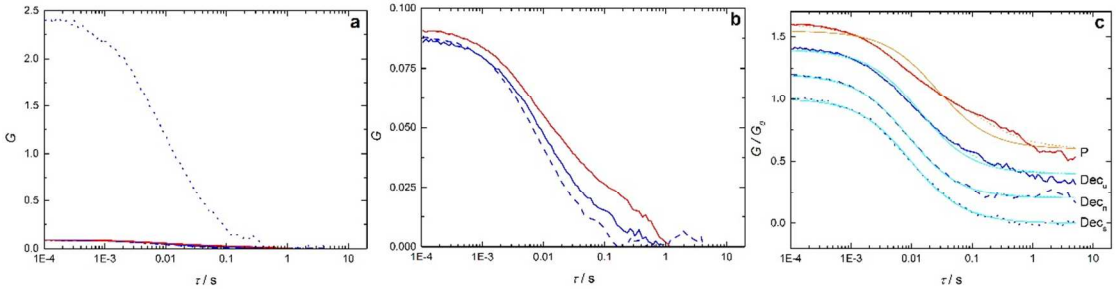

Figure 6. (a) FCS curves of the lipid SLBs obtained on differently cleaned glass slides and a zoom in **(b)**: cleaning with Piranha and subsequent rinsing with water (red), 15 min ultrasonic purification with Deconex 11 (blue) with subsequent 15 min ultrasonic purification with water (solid line), with subsequent rinsing with water (dashed line) and with subsequent dipping in water (insert, dotted line), respectively. **(c)** FCS curves normalized to 1 with the corresponding fits, either with the D_1 fit (solid line) or D_2 fit (dotted line). For better readability the curves are shifted along the y axis (P + 0.6, Dec_u + 0.4, Dec_n + 0.2).

Detergent and surface treatment	D_1 fit	D_2 fit			F-test
	D [$10^{-12}m^2s^{-1}$]	D_a [$10^{-12}m^2s^{-1}$] (a in %)	D_b [$10^{-12}m^2s^{-1}$]	D [$10^{-12}m^2s^{-1}$]	
P	1.57 ± 0.05	0.23 ± 0.04 (42 ± 3)	5.4 ± 0.8	3.3 ± 0.3	D_2
Dec_u	2.54 ± 0.08	3.8 ± 0.8 (78 ± 13)	0.5 ± 0.3	3.1 ± 0.3	D_2
Dec_n	3.9 ± 0.1	No meaningful result			D_1
Dec_s	3.5 ± 0.1	2.6 ± 0.7 (69 ± 33)	7.93 ± 5.2	4.26 ± 0.4	D_2

Table 1. Diffusion coefficients and the weighted average of the diffusion coefficients D_a and D_b of the SLBs on the differently cleaned glass slides obtained from the FCS curves in Graph 2 and the preferred model obtained from a F-test.

Treatment with strongly acidic or basic detergents leads to change in ζ-potential at the surface.[34] Based on our results, we hypothesized, that it is only partially reversed by the rinsing with water, leading to a different attraction of the headgroups of the lipids. Hence, the composition of the detergent or slight variations in the subsequent washing process can lead to minute variations in the surface properties, as we also observe in our measurements.

Therefore we strongly discourage the use of strongly basic or acidic detergents to ensure reproducible SLB formation. In contrast, we strongly recommend the use of oxygen plasma for the treatment of the glass slides. This procedure is increasing the hydrophilicity and the cleanliness of the glass, which leads to a stable polar interaction with the lipid headgroups. By comparing measurements on different glass slides, we can state, that this cleaning procedure leads to highly reproducible glass surfaces (not shown here).

3.2.2 Temperature dependent pH of buffers and pkA of lipids

Due to observations that the storage temperature of the vesicle suspension influences the SLB properties we investigated this phenomenon in detail. For SLBs from DOPC/DOPS 65:35 clearly different FCS curves were observed for vesicle suspensions stored at 4 °C and at room temperature, respectively. While the D_1 fit is sufficient to describe the SLB formed from vesicle suspensions stored at room temperature, the D_2 fit has to be applied for the bilayer obtained from vesicle suspensions stored at 4 °C (Fig. 7). This effect might be a result of the pK_a of DOPS in the SLB of 7.5[38] in combination with the significant pH dependency of Tris buffer on temperature (pH(4 °C) = 7.8, pH(20 °C) = 7.4).[39] The vesicles from the cold vesicle suspension bind to the glass surface prior to temperature equilibration. Due to the pH change of the buffer during temperature equilibration, the charge of DOPS is supposed to change as well. While it can be compensated by the bulk solution for the upper layer, the volume of the aqueous layer between glass and bottom layer is too small for a full compensation. This may lead to charge differences in the two layers of the SLB and therefore a different behaviour of the two leaflets.

To proof, that the observed heterogeneous membrane fluidity is a result of different fluidity of the upper and lower lipid layer, a bilayer was built up from a vesicle suspension stored at 4 °C, labelled with CellMask. CellMask is a dye intercalating in membranes and lipid bilayers, after the layers have been formed. It is not penetrating the membrane, but only labelling the leaflet it is in contact with. Hence, only one layer is specifically labelled. In this case, the outer shell of the vesicles is labelled, which is later the bottom layer of the SLB. Hence, the motion in only one layer is analysed with FCS. The FCS analysis shows, that the D_1 fit is sufficient (Fig. 7c) and hence the diffusion inside one layer is homogeneous. Therefore it can be concluded that the observed difference is caused by the difference between the two layers.

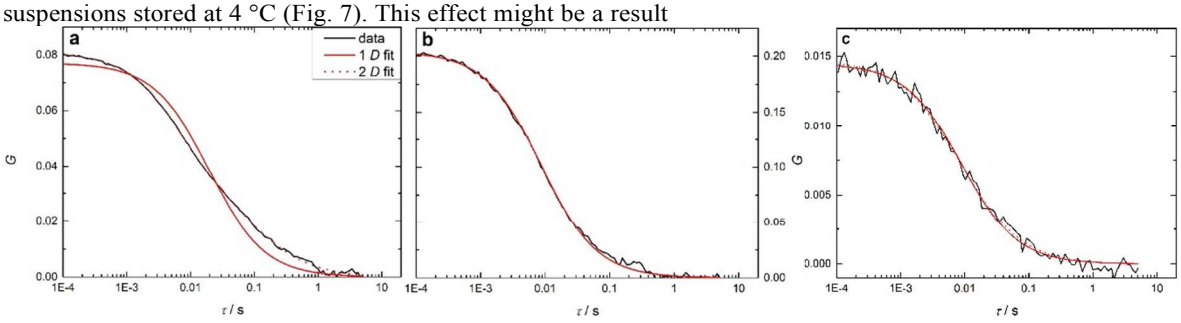

Figure 7. Data and corresponding fits of lipid SLBs formed from a vesicle suspension stored at 4 °C **(a)**, a vesicle suspension stored at room temperature **(b)** and a vesicle suspension stored at 4 °C labelled with Cellmask **(c)** on a plasma cleaned glass slide.

Lipid/Chol	DOPC/DOPS	SLB	*t*/min	D_{rel}
66:33	100:0	inhomogeneous	undefined	variable
80:20	100:0	inhomogeneous	undefined	variable
100:0	65:35	homogeneous	11	1
80:20	**65:35**	**homogeneous**	**15**	**0.47**
70:30	65:35	homogeneous	30	0.35

Table 2. Composition of the lipid mixtures (mixture closed to natural composition in bold[26]) and the corresponding properties of the SLB: the homogeneity, steady state incubation time t and diffusion coefficient D relative to the cholesterol free SLB.

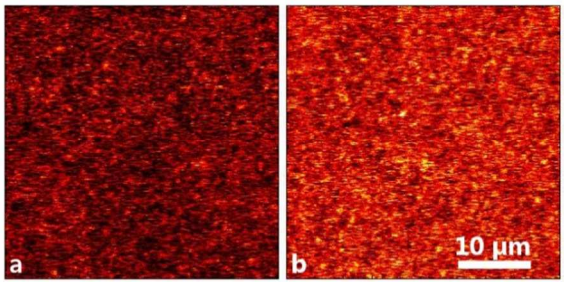

Figure 8. SAF scans of the SLBs formed out of DOPC/DOPS 65:35 with 20 % Cholesterol **(a)** and 30 % Cholesterol **(b)** recorded directly after changing the buffer to PBS.

3.3 SLBs containing cholesterol

Cholesterol (Chol) is an important component to build up microdomains in a membrane, so called lipid rafts,[39,40] and therefore important to mimic a natural membrane. Hence, we investigated the influence of Cholesterol on the formation of different SLB systems including a mixture close to the natural composition of the nerve ending membrane[26](Table 2, bold).For DOPC/Chol mixtures the formation of heterogeneous SLBs was observed.

For all mixtures containing DOPS SLBs could be successfully formed with prolonged steady state incubation times (Table 2). Their homogeneity was confirmed by SAF (Fig. 8). Lowered diffusion coefficients of these systems suggest, that Cholesterol is able to restrict movement inside a membrane. This is in line with previous studies.[40,41]

As precedent in the literature, that Cholesterol is separating the lipids inside a membrane into ordered and disordered domains.[42] This separation into domains can be visualized in the FCS analysis by analysing the FCS data with an anomalous diffusion model.[43] This model is taking into account the hindrance of the movement of the lipids due to the domains and the ratio between the size of the domains and the detection volume. The influence of the domains on the mobility of the lipids is expressed by the anomaly factor α with $\alpha = 1$ for unhindered diffusion. In the case of the Cholesterol containing SLBs the anomaly factor α is decreasing with increasing Cholesterol content (Table 3). Hence, also the influence of domains is getting higher.

Lipid/Chol	α
100:0	0.96 ±0.017
90:10	0.91 ± 0.016
80:20	0.86 ± 0.076
70:30	0.83 ± 0.071

Table 3. Anomaly factor for SLBs with DOPC/DOPS 65:35 with different Cholesterol content.

3.4 SLBs from lipid extracts

Using the protocol presented here, also the formation of artificial SLBs from natural lipid extracts is possible. Hence, lipid bilayers with a fully natural composition can be established, *i.e.* a model is provided to investigate the SLB behaviour close to natural conditions. However, the SLB formation out of lipid extracts is more demanding than from DOPC/DOPS mixtures. In contrast to the simplified phospholipid mixtures, natural lipid extracts contain a broad variety of lipids, including Gangliosides, Cholesterol etc. Therefore the components do not only vary in the charge of the headgroups, but also in size, polarity and amphiphilicity. Furthermore, DOPC and DOPS exhibit a phase transition temperature of -17 °C and -11 °C, respectively.[41,44] The phase transition temperature of lipid extracts is typically above room temperature.[44,45] This has to be taken into account during preparation of the lipid vesicles and leads to altered properties and formation of the produced SLBs.

The SLB formation from a polar lipid extract (60 % phospholipids) and a total lipid extract (41 % phospholipids) of porcine brain were studied. In a first attempt, the lipids were dissolved in Tris buffer with Ca^{2+}. A full coverage of the glass with lipid vesicles could be obtained with the flow/steady state approach. The vesicle coverage is comparable to the one of DOPC/DOPS vesicles.

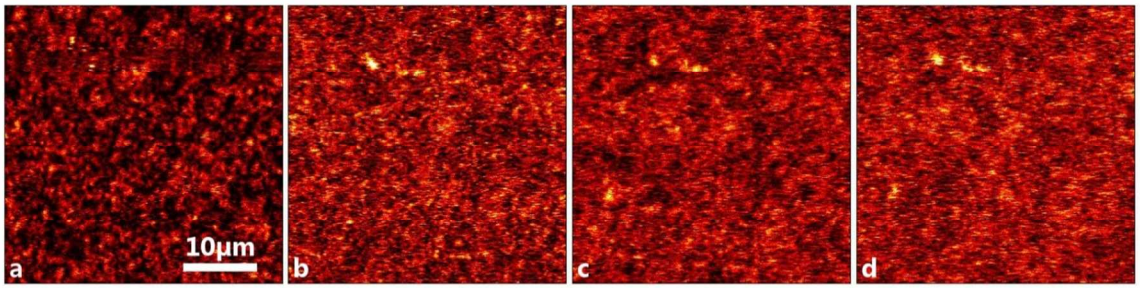

Figure 9. (a) Vesicle layer of the polar lipid extract in Tris buffer + Ca^{2+} before supporting flow, **(b)** SLB 20 min after applying flow, **(c)** SLB after washing with Tris buffer + Ca^{2+} and **(d)** after washing with Tris buffer + EDTA.

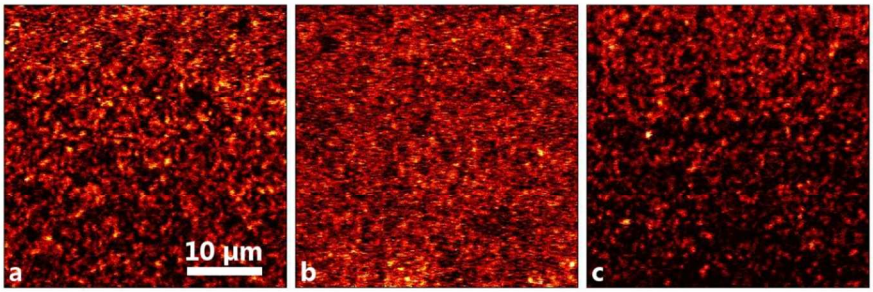

Figure 10. (a) Coexistence of a bilayer patch (upper part) and a vesicle layer (lower part) of the total lipid extract in Tris buffer + Ca^{2+}, **(b)** image of a full bilayer patch, which is dissolved after 90 min **(c)**.

The SLB formation though is different for both extracts. In the case of the polar lipid extract a rupture of the vesicles has to be supported by flow after 2 h of vesicle deposition. After 20 min of additional flow incubation time, the bilayer is formed. The total time until the assembled SLB can be rinsed is 2 h 20 min. The corresponding scans are depicted in Fig. 9.

For formation of the SLB from a total lipid extract, the flow was also applied after 2 hours. After 4 hours of incubation first lipid bilayer patches were formed (Fig.10a, upper part). These patches coexist with the vesicle layer around (Fig. 10a, lower part). The formed bilayer patches are not stable under Tris buffer + Ca and the process for full SLB formation is extremely slow.Hence, before the remaining vesicles could rupture, these bilayer patches were already dissolved due to their instability in the presence of Ca^{2+}. In Fig. 10b such a vesicles patch is shown, which is dissolved after 90 min resulting in a vesicle layer again (Fig. 10c). Under these conditions a stable, complete SLB could not be achieved.

To achieve a better and faster rupture of the vesicles the protocol for the preparation of the lipid vesicles was changed. Instead of dissolving the lipids in Tris buffer with Ca^{2+}, the lipids were dissolved in water, extruded and then diluted with Tris buffer with Ca^{2+} to create osmotic pressure. This osmotic pressure leads to an instability of the vesicles and therefore a faster rupture.[39]

In case of the polar lipid extract, the SLB formation is comparable to the one of the SLB systems with a DOPS content up to 40 %, as only steady state incubation is needed. After 10 min of steady state incubation with the lipid vesicles, the SLB builds up spontaneously. While for the artificial DOPC/DOPS mixtures the transition between vesicle layer and SLB is smooth and the exact time point of the transition is hard to define, for the polar lipid extract this transition is very sharp (Fig. 11).

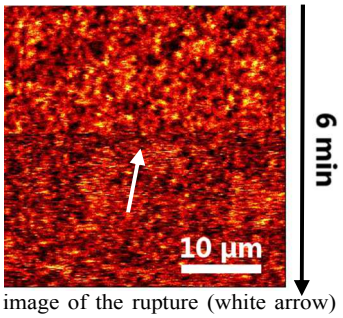

Figure 11. SAF image of the rupture (white arrow) of the polar lipid extract vesicle layer (upper part) into a homogeneous SLB (lower part).

Even after the exchange of the buffer solution with water in the extrusion step vesicles from total lipid extract do not spontaneously rupture under steady state conditions. Only shear forces created under flow successfully triggered SLB formation. As the vesicle coverage is increased with increasing steady-state time, the vesicle coverage at which the SLB is formed and hence its density can be controlled by varying the steady state incubation time (Fig. 12 and 13). Due to the higher vesicle coverage at higher steady state times the SLB formation is easier in this case and therefore the necessary flow incubation time shorter (Fig. 12a). Only at steady state incubation times over 140 min incomplete SLB formation is observed. Bilayer patches occur, which get dissolved and therefore lead to a less dense SLB, the same phenomenon as for the total lipid extract vesicles extruded with Tris buffer with Ca^{2+}.

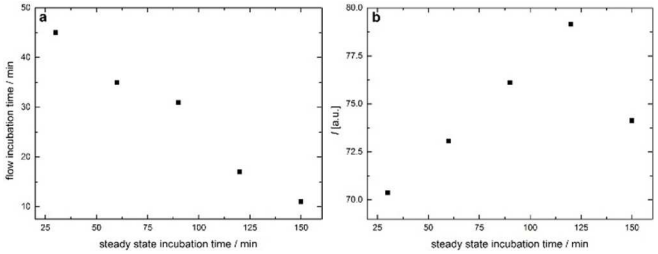

Figure 12. (a) Flow incubation time until vesicle rupture of the total lipid extract is reached plotted against the steady state incubation time and **(b)** averaged fluorescence intensity over one image taken directly after SLB formation.

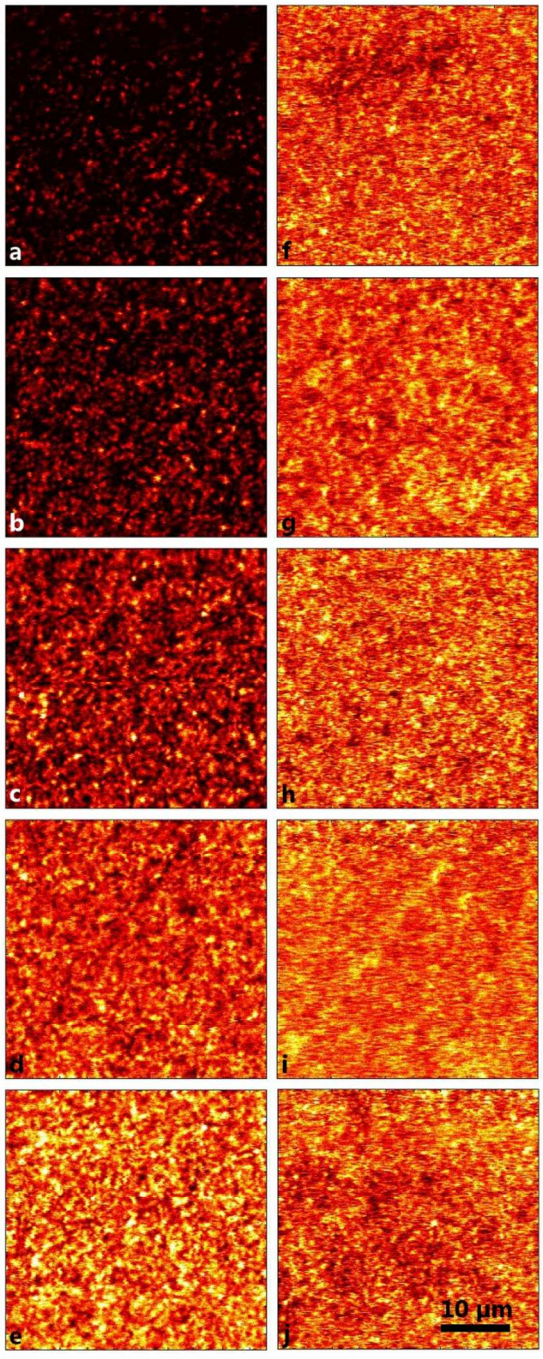

Figure 13. Total lipid vesicle layer after 30 min **(a)**, 60 min **(b)**, 90 min **(c)**, 120 min **(d)** and 150 min **(e)** under steady state incubation and the corresponding SLBs directly after their formation **(f-j)**.

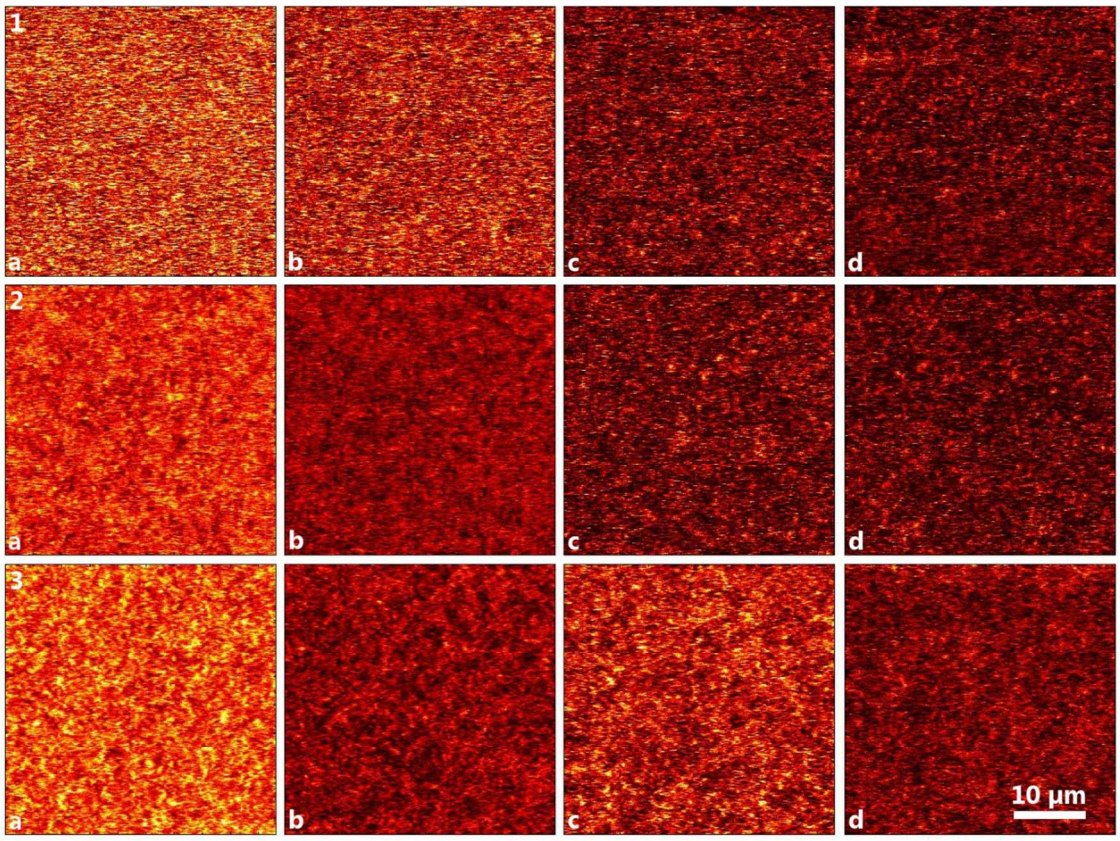

Figure 14. Scan over long time of SLBs built up from DOPC/DOPS 65:35 **(line 1)**, polar lipid extract **(line 2)** and total lipid extract **(line 3)**. Scans were taken 7 min **(a)**, 17 h **(b)**, 4 days **(c)** and 7 days **(d)** after changing to PBS buffer.

3.5 long-time stability of SLBs

For several applications a long-term stability of the SLB is desirable. So far, to our knowledge, this is the first report, that provides SLB stability for more than two hours, especially at high DOPS content. As an example, a SLB with 65:35 DOPC/DOPS was tested, as this is closest to physiological conditions. We also tested the SLBs from polar as well as total lipid extract. All three systems showed an extremely high long-term stability. Even after 4 days under flow the SLB was still stable. Only after one week first defects were getting visible, but the SLB structure was still existing (Fig. 14).
While in the other figures all images had the same intensity range, for the long-time experiments, the images show different intensity scales to visualize the homogeneity. To show the decrease in fluorescence intensity, which is caused by photobleaching as well as thinning of the SLB (for pure photobleaching the effect is too strong), the intensities over the time range of 7 days are depicted in Fig. 15. After two days the equilibrium density is reached and is highest for the total lipid extract, which also shows the best homogeneity after long time (Fig.14).

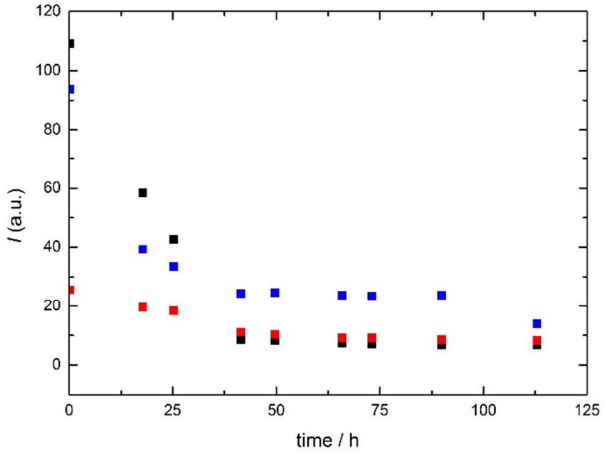

Figure 15. Average intensity of the scans over time for SLBs made from polar lipid extract **(black)**, total lipid extract **(blue)** and DOPC/DOPS 65:35 **(red)**.

Conclusions

In summary, we reported the assembly of long-term stable SLBs from various lipid mixtures including artificial DOPC/DOPS systems – also with cholesterol – and natural lipid extracts. Especially with the use of natural lipid extracts, we provide an interesting starting point for new biophysical and biosensing applications of SLBs. We developed a defined flow/steady-state sequence that ensures the reproducible formation of a homogeneous SLB. By using SAF microscopy,

we could clearly show, that under certain conditions the leaflets of the bilayer behave differently due to interaction of the bottom layer with the substrate. Crucial parameters for the SLB formation have been investigated in-depth and optimum conditions were extracted from the results. We discussed in detail the importance of the pre-treatment of the support as well as handling of the lipid suspensions. As a result, we could show a homogeneous SLB with the lipids in the two layers moving equally. By introducing a washing step with EDTA we were able to enhance the homogeneity and the stability of the bilayer reaching stabilities over seven days on glass supports. To the best of our knowledge, this is the first report of SLBs containing up to 70% DOPS or natural lipid extracts with this high homogeneity and long-term stability.

Acknowledgements

Financial support by the Swiss National Science Foundation (Grant 200020_140402) is gratefully acknowledged.

Notes and references

[a] Department of Chemistry, University of Zurich, Winterthurerstrasse 190, 8057 Zurich, Switzerland, isabelle.moeller@chem.uzh.ch.

[b] Department of Chemistry, University of Zurich, Winterthurerstrasse 190, 8057 Zurich, Switzerland, +41 44 63 54451, sseeger@chem.uzh.ch

References

1. C. Steinem, A. Janshoff, W.-P. Ulrich, M. Sieber and H.-J. Galla, *Biochimica et Biophysica Acta (BBA) - Biomembranes*, 1996, **1279**(2), 169.
2. E. Jo, J. McLaurin, C. M. Yip, P. St. George-Hyslop and P. E. Fraser, *Journal of Biological Chemistry*, 2000, **275**(44), 34328.
3. M. Rabe, A. Soragni, N. P. Reynolds, D. Verdes, E. Liverani, R. Riek and S. Seeger, *ACS Chem. Neurosci.*, 2012, **4**(3), 408.
4. N. P. Reynolds, A. Soragni, M. Rabe, D. Verdes, E. Liverani, S. Handschin, R. Riek and S. Seeger, *J. Am. Chem. Soc.*, 2011, **133**(48), 19366.
5. H. Hahl, I. Moller, I. Kiesel, S. Campioni, R. Riek, D. Verdes and S. Seeger, *ACS Chem Neurosci*, 2015.
6. E.-K. Sinner and W. Knoll, *Current Opinion in Chemical Biology*, 2001, **5**(6), 705.
7. N. S. Hatzakis, V. K. Bhatia, J. Larsen, K. L. Madsen, P.-Y. Bolinger, A. H. Kunding, J. Castillo, U. Gether, P. Hedegard and D. Stamou, *Nat Chem Biol*, 2009, **5**(11), 835.
8. A. Samad, Y. Sultana and M. Aqil, *Curr Drug Deliv*, 2007, **4**(4), 297.
9. A. S. Ladokhin, S. Jayasinghe and S. H. White, *Analytical Biochemistry*, 2000, **285**(2), 235.
10. A. H. Kunding, M. W. Mortensen, S. M. Christensen and D. Stamou, *Biophysical Journal*, 2008, **95**(3), 1176.
11. A. Granéli, J. Rydström, B. Kasemo and F. Höök, *Langmuir*, 2003, **19**(3), 842.
12. E. Briand, M. Zäch, S. Svedhem, B. Kasemo and S. Petronis, *The Analyst*, 2010, **135**(2), 343.
13. S. Chiantia, N. Kahya and P. Schwille, *Langmuir the ACS journal of surfaces and colloids*, 2005, **21**(14), 6317.
14. L. K. Tamm and H. M. McConnell, *Biophysical Journal*, 1985, **47**(1), 105.
15. H. P. Wacklin, *Langmuir the ACS journal of surfaces and colloids*, 2011, **27**(12), 7698.
16. G. J. Hardy, R. Nayak, S. M. Alam, J. G. Shapter, F. Heinrich and S. Zauscher, *Journal of materials chemistry*, 2012, **22**(37), 19506.
17. P. S. Cremer and S. G. Boxer, *J. Phys. Chem. B*, 1999, **103**(13), 2554.
18. N.-J. Cho, S.-J. Cho, K. H. Cheong, J. S. Glenn and C. W. Frank, *Journal of the American Chemical Society*, 2007, **129**(33), 10050.
19. Zasadzinski, J. A. N., C. A. Helm, M. L. Longo, A. L. Weisenhorn, Gould, S. A. C. and P. K. Hansma, *Biophysical Journal*, 1991, **59**(3), 755.
20. P. Nollert, H. Kiefer and F. Jähnig, *Biophysical Journal*, 1995, **69**(4), 1447.
21. C. A. Keller and B. Kasemo, *Biophysical Journal*, 1998, **75**(3), 1397.
22. I. Reviakine, W. Bergsma-Schutter and A. Brisson, *Journal of Structural Biology*, 1998, **121**(3), 356.
23. A. Mashaghi, M. Swann, J. Popplewell, M. Textor and E. Reimhult, *Anal. Chem.*, 2008, **80**(10), 3666.
24. R. P. Richter, N. Maury and A. R. Brisson, *Langmuir*, 2004, **21**(1), 299.
25. R. Richter, A. Mukhopadhyay and A. Brisson, *Biophysical Journal*, 2003, **85**(5), 3035.
26. A. P. Smith and H. H. Loh, *Life Sciences*, 1979, **24**(1), 1.
27. J. Ries, T. Ruckstuhl, D. Verdes and P. Schwille, *Biophysical Journal*, 2008, **94**(1), 221.
28. J. Enderlein, T. Ruckstuhl and S. Seeger, *Appl. Opt.*, 1999, **38**(4), 724.
29. T. Ruckstuhl, M. Rankl and S. Seeger, *Biosensors and Bioelectronics*, 2003, **18**(9), 1193.
30. C. M. Winterflood, T. Ruckstuhl, D. Verdes and S. Seeger, *Phys. Rev. Lett.*, 2010, **105**(10), 108103.
31. J. Adler and I. Parmryd, *Cytometry. Part A the journal of the International Society for Analytical Cytology*, 2010, **77**(8), 733.
32. E. Kalb, S. Frey and L. K. Tamm, *Biochimica et Biophysica Acta (BBA) - Biomembranes*, 1992, **1103**(2), 307.
33. J.-M. Nam, P. M. Nair, R. M. Neve, J. W. Gray and J. T. Groves, *ChemBioChem*, 2006, **7**(3), 436.
34. B. J. Kirby and E. F. Hasselbrink, *ELECTROPHORESIS*, 2004, **25**(2), 187.
35. H. J. Motulsky and L. A. Ransnas, *The FASEB Journal*, 1987, **1**(5), 365.
36. M. Przybylo, J. Sýkora, J. Humpolíčková, A. Benda, A. Zan and M. Hof, *Langmuir*, 2006, **22**(22), 9096.
37. M. Hetzer, S. Heinz, S. Grage and Bayerl, T. M., *Langmuir*, 1998, **14**(5), 982.
38. F. C. Tsui, D. M. Ojcius and W. L. Hubbell, *Biophysical Journal*, 1986, **49**(2), 459.
39. E. Reimhult, F. Höök and B. Kasemo, *Langmuir*, 2002, **19**(5), 1681.
40. D. A. Brown and E. London, *J. Membrane Biol.*, 1998, **164**(2), 103-114.

41. U. Cogan, M. Shinitzky, G. Weber and T. Nishida, *Biochemistry*, 1973, **12**(3), 521.
42. M. C. Rheinstädter and O. G. Mouritsen, *Current Opinion in Colloid & Interface Science*, 2013, **18**(5), 440.
43. L. Wawrezinieck, H. Rigneault, D. Marguet and P.-F. Lenne, *Biophysical Journal*, 2005, **89**(6), 4029.
44. [Der Titel "#29" kann nicht dargestellt werden – Die Vorlage "Literaturverzeichnis - Internetdokument - (Standardvorlage)" beinhaltet nur Felder, welche bei diesem Titel leer sind.]
45. R. Koynova and R. C. MacDonald, *Biochimica et Biophysica Acta (BBA) - Biomembranes*, 2007, **1768**(10), 2373.

We show the assembly of reproducible, long-term stable, homogeneous solid supported lipid bilayers under flow conditions by the vesicle deposition method from various artificial and natural lipid mixtures.